Performance, Complexity, and Receiver Design for Code-Aided Frame Synchronization in Multipath Channels

Daniel J. Jakubisin, *Student Member, IEEE* and R. Michael Buehrer, *Senior Member, IEEE*

***Abstract*—Next generation wireless communications systems are pushing the limits of both energy efficiency and spectral efficiency. This presents a challenge at the receiver when it comes to accomplishing tasks such as synchronization, channel estimation, and equalization and has motivated the development of code-aided iterative receiver algorithms in the technical literature. In this paper, we focus on the task of frame synchronization. While previous work has predominately assumed an additive white Gaussian noise channel, we develop code-aided frame synchronization algorithms for multipath channels. An iterative receiver is presented which integrates frame synchronization with iterative channel estimation, equalization, demodulation, and decoding. The receiver design includes a novel frame pre-processing stage to reduce the complexity of the proposed receiver. The complexity and performance of the proposed receiver is compared with that of a receiver based on conventional synchronization. The results demonstrate that the proposed receiver is capable of achieving a gain of up to 3 dB while increasing complexity by only 20%.**

***Index Terms*—Frame synchronization, code-aided, iterative receivers, multipath channels, sum product algorithm, expectation-maximization algorithm.**

I. Introduction

NEXT generation wireless communications systems are pushing the limits of both energy efficiency and spectral efficiency. Energy efficiency is aided by advanced error correction codes while spectral efficiency is aided by multiple-input multiple-output (MIMO) transmission, higher order modulations, adaptive rate control, orthogonal frequency-division multiplexing (OFDM), and the reduction of training overhead. However, these advances present a challenge at the receiver when it comes to accomplishing tasks such as synchronization, channel estimation, and equalization. This has motivated the development of code-aided algorithms in the technical literature (see, for example, [3]–[6]). These algorithms are generally iterative—making use of probabilistic information from the decoder to improve the performance of earlier receiver tasks.

Frame synchronization refers to the acquisition of the start time of a frame of transmitted data. Accurate synchronization is particularly important for block codes such as turbo codes and low-density parity-check (LDPC) codes where the information of the whole frame is lost if the frame start time is incorrectly estimated. Frame synchronization is traditionally accomplished by adding a sync word as a preamble to the frame and correlating the received signal with this known sequence [7]. The complexity of the correlation technique is low, but it is sub-optimal in terms of frame synchronization error probability. Optimal maximum *a posteriori* probability (MAP) frame synchronization for *uncoded data* is derived for binary phase-shift keying (BPSK) in [8] and for higher-order modulations in [9] where significant gains in frame synchronization performance are shown when compared to the correlation technique.

MAP frame synchronization for *coded data* requires marginalization over the entire set of codewords. Herzet and Vandendorpe recognized that the sum-product algorithm is capable of efficiently performing the desired marginalization over the coded data when the factor graph of the joint probability distribution is acyclic [10]. In general, however, marginalization over the entire set of codewords is too complex and thus a number of code-aided frame synchronization methods have been proposed in the literature [11]–[24]. Frame synchronization is performed in [23], [24] by computing the syndrome posterior probability (SPP) of the code's parity check relations. This same approach is applied to blind code recognition in [25]. Code-aided frame synchronization based on the expectation-maximization (EM) algorithm is presented in [17]. Further theoretical justification for the EM-motivated algorithm is provided in [18] where it is shown to be an approximation to MAP hypothesis testing (HT). Frame synchronization based on free energy minimization is proposed in [19] taking advantage of recent connections between belief propagation and free energy minimization from statistical physics [26].

In the case of uncoded signals, likelihood based frame synchronization is derived for flat-fading channels in [27] and frequency-selective channels in [28]. However, previous work on code-aided frame synchronization predominately assumes an additive white Gaussian noise (AWGN) channel. Two exceptions include [13] and [20] which develop frame synchronization based on decoder state estimation for convolutional codes and provide results for flat-fading and frequency-selective channels, respectively. Moreover, previous work on code-aided frame synchronization has typically assumed knowledge of the other channel parameters and the noise power.

Code-aided frame synchronization techniques require processing each potential frame offset individually and the processing requires decoding [11], [15], [17], [18] or a decoding-

This work has been presented in part at the 2014 IEEE Wireless Commun. and Netw. Conf. (WCNC) [1] and the IEEE 15th Workshop Signal Process. Advances Wireless Commun. (SPAWC) [2]. The authors are with the Bradley Department of Electrical and Computer Engineering, Virginia Tech, Blacksburg, VA 24061, USA. (e-mail: {djj,buehrer}@vt.edu).

like operation [10], [16], [19], [21]–[24]. Therefore, the complexity of the receiver as a whole scales linearly with the number of frame offsets considered by the code-aided synchronizer. Robertson proposed a two-stage frame synchronizer, referred to as list synchronization, in which a low-complexity decision rule is used to obtain a list of the most likely frame offsets and then this list is processed by a high-complexity decision rule [11]. Other papers that have applied the list synchronization method in their analysis include [13], [15]. However, parameters of the list synchronization method (for instance, the size of the list) are determined through simulation. What is lacking with the list synchronization method is the ability to choose the optimal number of candidate frame offsets to be considered by the high complexity decision rule.

In this paper, the problem of frame synchronization is considered for coded signals in *multipath channels*. We consider the case in which the channel is not known *a priori*, and develop an iterative receiver structure for frame synchronization, channel estimation, equalization, demodulation, and decoding. The paper expands upon the receiver structure and pre-processing stage developed in the authors previous work, which only considered the AWGN channel [1]. In contrast to Robertson's list synchronizer, the pre-processing stage uses a Bayesian technique to select, on a frame-by-frame basis, the subset of frame offsets to be processed by a code-aided frame synchronizer. The proposed technique selects the minimum number of offsets for a given target performance by computing the highest posterior density (HPD) region of the frame distribution. Numerical results are provided to characterize the expected number of frame offsets in the HPD region because the computational complexity of code-aided frame synchronization is proportional to the number of frame offsets which must be processed.

Two code-aided frame synchronization methods are developed for multipath channels. The first algorithm, based on the SPP method, is designed to have a low-complexity. The second algorithm, based on the EM method, is designed to be an iterative approximation to joint MAP synchronization and data detection. In the case of unknown channel parameters, code-aided frame synchronization is generalized to code-aided hypothesis testing of the frame offset and phase ambiguity. We consider two implementations of the EM-based method in the iterative receiver. The first, HT/ECM, performs EM-based code-aided hypothesis testing of the frame offset and phase ambiguity while iteratively re-estimating the remaining channel parameters using the expectation-conditional maximization (ECM) algorithm [29]. The second, HT, performs EM-based code-aided hypothesis testing without re-estimating the remaining parameters in order to reduce complexity.

This paper also extends the authors previous work in [2] by exploring the complexity-performance trade-off of code-aided frame synchronization in multipath channels. Regions of signal-to-noise ratio (SNR) are identified for which code-aided frame synchronization provides an improvement in performance while maintaining a complexity within a factor of $2\times$ that of conventional techniques. The performance of the receiver is demonstrated in a scenario in which the proposed receiver achieves a gain of up to 3 dB with a complexity increase of only 20%. We also show that code-aided frame synchronization may be reliably performed at SNR values below that required for decoding. This is important, for example, to support acknowledgment (ACK)/non-acknowledgment (NACK) and hybrid automatic repeat request (hybrid ARQ) protocols or to achieve reliable synchronization in a collaborative communications scenario where multiple receivers may cooperate to decode a signal at low SNR.

In summary, the contributions of this paper are as follows:

- Development of code-aided frame synchronization for multipath channels
- Development of a novel frame pre-processing stage to allow a trade-off between performance and complexity
- Design of an iterative receiver for frame synchronization, channel estimation, equalization, demodulation, and decoding
- Analysis of the complexity-performance trade-off in order to identify regions where code-aided frame synchronization is beneficial
- Analysis of code-aided frame synchronization performance at SNR values below that required for decoding.

This paper is organized as follows. The system model is given in Section II and MAP frame synchronization is reviewed in Section III. A brief overview of the proposed receiver structure is presented in Section IV. A novel frame pre-processing stage which guarantees a maximum probability of excluding the true frame offset is presented in Section V. In Section VI, the SPP and EM-based code-aided frame synchronization techniques are developed for multipath channels and numerical results are provided in Section VII. The receiver is developed in Section VIII for an unknown channel, including the HT/ECM and HT receivers, and numerical results are presented. Finally, the paper is concluded in Section IX.

II. System Model

A burst transmission scheme is considered in this paper. At the transmitter an error correction code is applied to a sequence of N_b information bits $\mathbf{b}$ to produce a sequence of N_c coded bits $\mathbf{c}$. Subsequently, the coded bits are modulated using a digital phase-amplitude modulation to form a complex sequence of coded data symbols denoted by $\mathbf{a} = [a_0, \ldots, a_{N_a-1}]^{\mathrm{T}}$ with length N_a. The symbol alphabet is given by the set $\{m_i\}_{i=1}^{M}$, where M is the order of the modulation, and is normalized to unit average power (i.e., $\frac{1}{M}\sum_{i=1}^{M}|m_i|^2 = 1$). A frame is constructed from the concatenation of a sync word and the coded data sequence as given by $\mathbf{x} = [\mathbf{s}^{\mathrm{T}}\mathbf{a}^{\mathrm{T}}]^{\mathrm{T}}$ where $\mathbf{s} = [s_0, \ldots, s_{N_s-1}]^{\mathrm{T}}$ is the sync word with length N_s. The frame length is given by $K = N_s + N_a$.

The low-pass equivalent of the transmitted frame is given by

$$q(t) = \sum_{k=0}^{K-1} x_k p(t - kT), \tag{1}$$

where $p(t)$ is a real valued pulse with unit energy and T is the symbol period. The multipath channel is modeled with a conventional tapped delay line with tap spacing equal

to T [30]. The low-pass equivalent of the channel impulse response is given by

$$h(t) = \sum_{l=0}^{L-1} h_l \delta(t - lT - \tau), \tag{2}$$

where h_l are the complex channel coefficients for each of the L resolvable paths, and τ is a time delay. Let the delay be separated into an integer multiple of the symbol period η (i.e., the frame offset) and a fractional multiple of the symbol period ϵ such that $\tau = (\eta+\epsilon)T$ where $0 \leq \epsilon < 1$. The low-pass equivalent of the received signal is given by

$$r(t) = \sum_{l=0}^{L-1} h_l \sum_{k=0}^{K-1} x_k p(t - (k + l + \eta + \epsilon)T) + w(t), \tag{3}$$

where $w(t)$ is a spectrally-white complex Gaussian random process representing noise. At the output of the matched filter, the received signal is given by

$$y(t) = r(t) * p(-t) = \sum_{l=0}^{L-1} h_l \sum_{k=0}^{K-1} x_k g(t - (k + l + \eta + \epsilon)T) + v(t), \tag{4}$$

where $g(t) = p(t) * p(-t)$ is a Nyquist pulse (for example, a raised cosine pulse) and $v(t) = \int_{-\infty}^{\infty} w(\xi)p(\xi - t)d\xi$ is filtered noise. When the symbol timing ϵ is known, samples y_n of the matched filter output may be taken at $t = (n + \epsilon)T$ as given by

$$y_n = y((n + \epsilon)T) = \sum_{l=0}^{L-1} h_l x_{n-l-\eta} + v_n, \tag{5}$$

where x_i is non-zero for indexes $0 \leq i \leq K - 1$ and $\{v_n\}_{n=0}^{N-1}$ are independent and identically distributed (iid) circularly-symmetric complex Gaussian random variables with variance given by σ^2. Let the domain of the frame offset be given by $\eta \in \{0, 1, \ldots, H - 1\}$ where H is assumed to be large due to prior uncertainty in the start time of the frame. The vector of samples of the matched filtered signal is denoted by $\mathbf{y} = [y_0, \ldots, y_{N-1}]^{\mathrm{T}}$ and has length $N = K + H + L - 2$ to account for the length of the frame, the multipath channel, and all possible frame offsets. Throughout the paper, SNR is defined as the ratio between the instantaneous power of the multipath channel and the noise power as expressed by

$$\mathrm{SNR} = \frac{\sum_{l=0}^{L-1} |h_l|^2}{\sigma^2}. \tag{6}$$

III. MAP Frame Synchronization

Following convention, we define the optimum frame synchronizer to be the estimator which maximizes the probability of selecting the correct frame offset [8]. Given an observation of the received signal $\mathbf{y}$, this estimator is the one which maximizes the posterior probability of the frame offset $p(\eta|\mathbf{y})$. According to Bayes' rule the posterior probability is given by

$$p(\eta|\mathbf{y}) = \frac{p(\mathbf{y}|\eta)p(\eta)}{p(\mathbf{y})} \propto p(\mathbf{y}|\eta)p(\eta). \tag{7}$$

The distribution $p(\mathbf{y}|\eta)$ is expressed as the marginalization of the joint distribution $p(\mathbf{y}, \mathbf{x}|\eta)$ over $\mathbf{x}$ producing the following MAP estimator:

$$\hat{\eta}_{\mathrm{MAP}} = \underset{\eta \in \{0,\ldots,H-1\}}{\arg\max} \sum_{\mathbf{x}} p(\mathbf{y}|\mathbf{x}, \eta)p(\mathbf{x})p(\eta), \tag{8}$$

where $\sum_{\mathbf{x}}$ denotes marginalization over the domain of $\mathbf{x}$.

Given knowledge of the channel and noise parameters, the likelihood function for observation of the symbol-synchronous samples from (5) is given by

$$\begin{aligned} p(\mathbf{y}|\mathbf{x}, \eta) \propto & \prod_{i=0}^{\eta-1} \exp\left\{-\frac{1}{\sigma^2}|y_i|^2\right\} \\ & \cdot \prod_{i=0}^{L-2} \exp\left\{-\frac{1}{\sigma^2}\left|y_{i+\eta} - \sum_{l=0}^{i} h_l x_{i-l}\right|^2\right\} \\ & \cdot \prod_{i=L-1}^{K-1} \exp\left\{-\frac{1}{\sigma^2}\left|y_{i+\eta} - \sum_{l=0}^{L-1} h_l x_{i-l}\right|^2\right\} \\ & \cdot \prod_{i=K}^{K+L-2} \exp\left\{-\frac{1}{\sigma^2}\left|y_{i+\eta} - \sum_{l=i-K+1}^{L-1} h_l x_{i-l}\right|^2\right\} \\ & \cdot \prod_{i=K+L+\eta-1}^{N-1} \exp\left\{-\frac{1}{\sigma^2}|y_i|^2\right\}. \end{aligned} \tag{9}$$

In (9), the first and fifth products are distributions on the noise-only samples before and after the frame, respectively. The second, third, and fourth products are distributions on the signal (with intersymbol interference due to multipath) and noise. The second and fourth products take into account the effects of multipath at the beginning and end of the frame, respectively. In order to simplify the notation, let $\alpha_i = \max(i - K + 1, 0)$ and $\beta_i = \min(i, L - 1)$ represent lower and upper limits, respectively, on the summation of the multipath terms within the exponential functions of (9). Further, recognizing that the term $\prod_{i=0}^{N-1} \exp\left\{-\frac{1}{\sigma^2}|y_i|^2\right\}$ is a proportionality constant with respect to the frame offset, the likelihood function can be simplified as follows:

$$\begin{aligned} p(\mathbf{y}|\mathbf{x}, \eta) \propto \prod_{i=0}^{K+L-2} \exp\Bigg\{ & \frac{2}{\sigma^2}\Re\left[y_{i+\eta}^* \sum_{l=\alpha_i}^{\beta_i} h_l x_{i-l}\right] \\ & - \frac{1}{\sigma^2}\left|\sum_{l=\alpha_i}^{\beta_i} h_l x_{i-l}\right|^2 \Bigg\}. \end{aligned} \tag{10}$$

Returning to (8), the prior probability of the data sequence $p(\mathbf{x})$ can be decomposed into a product of prior probabilities for the sync word and the coded symbols $p(\mathbf{s})p(\mathbf{a})$. The sync word is deterministic (i.e., $p(\mathbf{s}) = 1$ for the true sync word and is zero for all other sequences). Since the prior probability $p(\mathbf{a})$ is zero for all symbol sequences which do not correspond to a valid codeword, the complexity of computing (8) is $O(2^{N_b})$, i.e., it scales with the number of codewords[1]. In the case of an uncoded signal, the complexity is $O(M^L)$ due to the multipath

[1]The term O denotes the standard big O notation which is used to describe the asymptotic behavior of a function—in our case the number of computations as a function of the signal parameters.

terms in (10) and the marginalization can be performed using the Bahl-Cocke-Jelinek-Raviv (BCJR) algorithm [31].

The following three factors contribute to the complexity of the MAP estimator in (8):

- *The size of the search space* $\eta \in \{0, \ldots, H-1\}$*:* The time between burst transmission may create a large search space for the frame start time. A low complexity pre-processing stage is developed in Section V to address this challenge.
- *The exponential complexity of the marginalization:* As described above, the MAP estimator is too complex to implement. Therefore, in Section VI, we develop code-aided frame synchronization algorithms for multipath channels which approximate the MAP estimator.
- *The presence of unknown parameters:* The complex channel coefficients $\mathbf{h} = [h_0, \ldots, h_{L-1}]^{\mathrm{T}}$, the fractional (symbol) delay ϵ, and the noise power σ^2 are required for the pre-processing stage and code-aided algorithms developed in this paper. An extension of the work to the unknown channel case is given in VIII.

First, we provide a brief overview of the receiver structure in the following section.

IV. Receiver Design

In the proposed iterative receiver structure, shown in Fig. 1, frame synchronization is performed in two stages: (1) frame pre-processing and (2) code-aided frame synchronization. Coarse estimation of the symbol timing and channel parameters is performed prior to the frame pre-processing stage. In the frame pre-processing stage, an uncoded signal model is assumed in order to narrow the search for the frame offset to the HPD region. Code-aided frame synchronization is performed for each frame offset in the HPD region as represented by the duplicate receiver chains in Fig. 1. When the HPD region contains a single frame offset, this offset is selected without the need to perform code-aided frame synchronization. Further processing is performed on the iterative receiver chain corresponding to the selected frame offset (as shown by the shaded region in Fig. 1) in order to detect the information bits. In the iterative receiver, fine estimation of the continuous channel parameters (ϵ, $\mathbf{h}$, and σ^2) is accomplished with the ECM algorithm. The sum-product algorithm [32] is utilized to perform iterative, probabilistic equalization, demodulation, and decoding in order to compute posterior probabilities of the symbols and information bits used for fine channel estimation and data detection, respectively.

V. Pre-Processing Stage

The frame pre-processing stage shown in Fig. 1 is developed in this section. Due to the burst transmission scheme, we assume that the search space for the frame offset $\{0, \ldots, H-1\}$ is large. Instead of processing all frame offsets with a code-aided algorithm, a pre-processing stage identifies a subset $\mathcal{S}$ of the most probable frame offsets based on the assumption that the data is uncoded. The pre-processing stage modifies

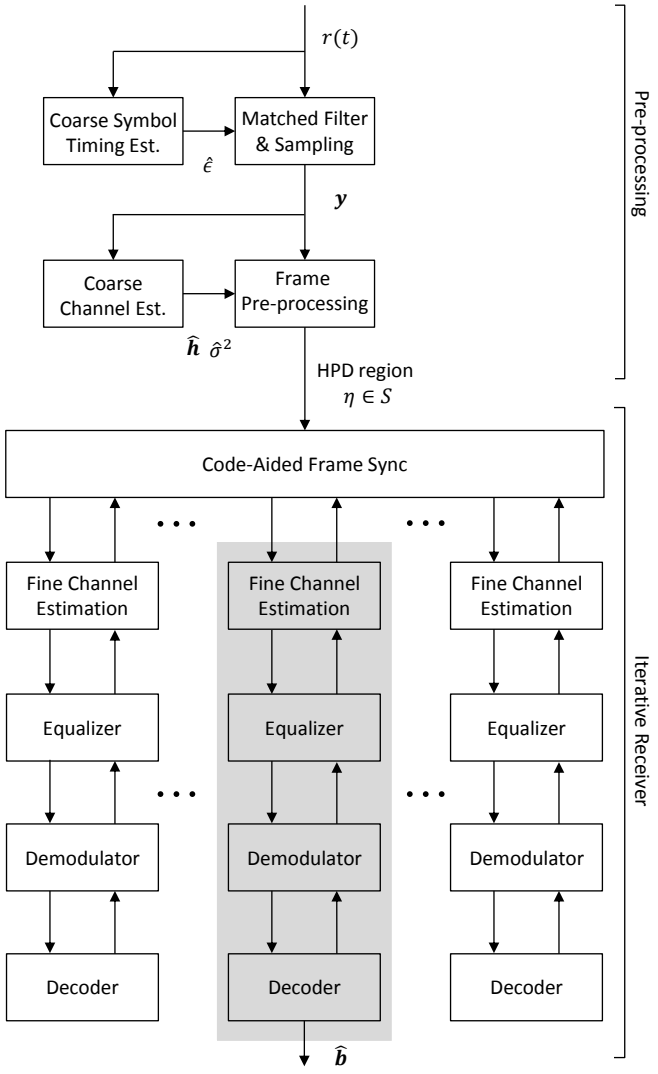

Fig. 1. Proposed iterative receiver design for implementing code-aided frame synchronization with a pre-processing stage.

the search space of the MAP estimator in (8) so that the approximate MAP estimate is given by

$$\hat{\eta}_{\mathrm{MAP}} \approx \arg\max_{\eta \in \mathcal{S}} \sum_{\mathbf{x}} p(\mathbf{y}|\mathbf{x}, \eta) p(\mathbf{x}) p(\eta). \tag{11}$$

A. HPD Region-Based Pre-Processing

Given a subset of the frame offsets denoted by $\mathcal{S}$ with size $|\mathcal{S}|$, we define P_{ex} to be the probability that the true offset has been excluded from $\mathcal{S}$ (i.e., $\eta_{true} \notin \mathcal{S}$). We desire to find the smallest subset for which the probability that the true offset is included in this set is greater than or equal to $(1 - P_{ex})$. This set is known as the highest posterior density (HPD) region. For example, to limit the probability of exclusion to $P_{ex} = 0.01$, the set of frame offsets $\mathcal{S}$ which must be processed by the code-aided method is given by the 0.99 HPD region. An example posterior distribution is shown in Fig. 2 where the 0.99 HPD region is shown with marker "x". In this example, the HPD region contains seven offsets: $\{15, 22, 23, 24, 25, 26, 27\}$. The number of offsets

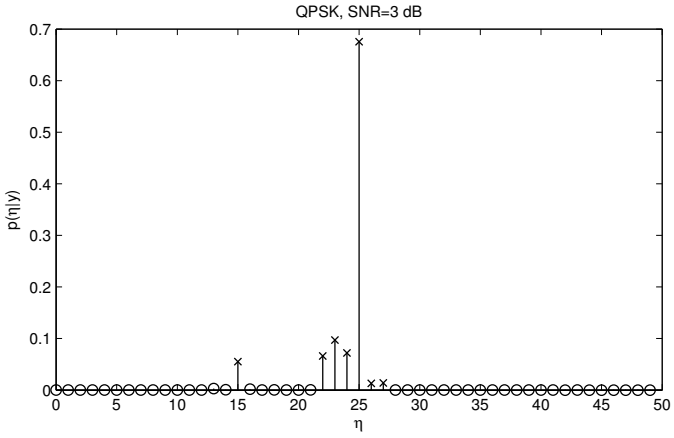

Fig. 2. Example posterior distribution and 0.99 highest posterior density region (shown with 'x') with true offset $\eta = 25$.

is dynamically chosen when determining the HPD region and, as seen in Fig. 2, the offsets need not be contiguous. Mathematically, we can express the $(1 - P_{ex})$ HPD region as the smallest set $\mathcal{S}$ such that

$$\sum_{\eta \in \mathcal{S}} p_{\text{uncoded}}(\eta|\mathbf{y}) \geq 1 - P_{ex}, \tag{12}$$

where p_{uncoded} denotes the distribution under the *uncoded* signal model. If $|\mathcal{S}| > 1$, the frame offsets contained in the HPD region are passed to the code-aided algorithm in order to make a reliable decision.

Using the HPD region allows the receiver to choose on a frame by frame basis how many and which frame offsets to process with the code-aided method. Subsequently, the number of frame offsets processed by the code-aided method is minimized for a specified P_{ex}. Note that the frame synchronization error rate (FSER) of the receiver will be lower-bounded by P_{ex} which will in turn lower bound the achievable frame error rate (FER) of data detection.

In the MAP estimator given in (8), the *a priori* distribution of the frame offset $p(\eta)$ is assumed to be uniform over the domain $\eta \in \{0, \ldots, H-1\}$. The prior on the coded symbols $p(\mathbf{a})$ is non-zero and uniform for all symbol sequences which correspond to valid codewords. However, under the assumption of iid data symbols (i.e., the assumption of an uncoded signal) the prior reduces to $\prod_{i=0}^{N_a-1} p(a_i)$ where $p(a_i)$ is assumed to be a uniform distribution. In the case of an AWGN channel (given by (5) with $L = 1$) the assumption of the uncoded signal model simplifies the posterior distribution to

$$p_{\text{uncoded}}(\eta|\mathbf{y}) \propto \prod_{i=0}^{N_s-1} \exp\left\{\frac{2}{\sigma^2}\Re\left[y_{i+\eta}^* h_0 s_i\right]\right\} \cdot \prod_{i=0}^{N_a-1} \sum_{a_i} \exp\left\{\frac{2}{\sigma^2}\Re\left[y_{i+\eta+N_s}^* h_0 a_i\right] - \frac{1}{\sigma^2}|h_0 a_i|^2\right\}, \tag{13}$$

where the computational complexity is $O(N_s + N_a M)$.

In the case of the multipath channel, the assumption of an uncoded signal model reduces the complexity of computing the posterior distribution to $O(N_s L + N_a M^L)$. The complexity is still exponential in the number of channel taps due to the second term in the likelihood function of (10): $\left|\sum_{l=\alpha_i}^{\beta_i} h_l x_{i-l}\right|^2$. By dropping these terms from the likelihood function and assuming an uncoded signal model, the complexity is further reduced. Although these terms are not functions of the frame offset η, they cannot be factored from the likelihood function because they appear within the summation over $\mathbf{x}$. Thus, their removal results in the following approximation of the likelihood function[2]:

$$p(\mathbf{y}|\mathbf{x}, \eta) \overset{\propto}{\sim} \prod_{i=0}^{K+L-2} \exp\left\{\frac{2}{\sigma^2}\Re\left[y_{i+\eta}^* \sum_{l=\alpha_i}^{\beta_i} h_l x_{i-l}\right]\right\}. \tag{14}$$

A similar approximation is used in [28] for frame synchronization of uncoded signals. Substituting (14) into the posterior distribution for uncoded signals and grouping the intersymbol interference (ISI) terms by symbol leads to the following approximate posterior distribution:

$$p_{\text{uncoded}}(\eta|\mathbf{y}) \overset{\propto}{\sim} \prod_{i=0}^{N_s-1} \exp\left\{\frac{2}{\sigma^2}\Re\left[s_i \sum_{l=0}^{L-1} y_{i+l+\eta}^* h_l\right]\right\} \cdot \prod_{i=0}^{N_a-1} \sum_{a_i} \exp\left\{\frac{2}{\sigma^2}\Re\left[a_i \sum_{l=0}^{L-1} y_{i+l+\eta+N_s}^* h_l\right]\right\}, \tag{15}$$

with computational complexity $O(N_s L + N_a M L)$. In the section that follows, (15) is shown to provide a good approximation to the posterior distribution for the purpose of computing the HPD region.

B. HPD Region Characterization

We desire to characterize the HPD region in order to evaluate the impact that the pre-processing stage has on the complexity of the receiver. The code-aided algorithms will process each frame offset in the HPD region. Thus, understanding the expected size of the HPD region provides insight into the complexity of the receiver. We also benchmark the performance by comparing the probability of exclusion P_{ex} of the HPD region with the FSER of the MAP estimate under the uncoded signal model (from now on referred to as the *uncoded MAP estimate*).

The mean number of frame offsets in the HPD region is determined through Monte Carlo simulation. We consider BPSK modulation and m-sequences of length 7, 15, 31, and 63 for the sync word. Since P_{ex} provides a lower bound on the FER of the receiver, we set $P_{ex} = 10^{-3}$ with the perspective that FERs of 10^{-2} to 10^{-3} are typical for wireless communication systems in multipath channels. In the case of multipath, the results are averaged over realizations of a $L = 4$ tap channel drawn from complex Gaussian random variables where the relative power in each tap is given by $[0.644, 0.237, 0.087, 0.032]$. The results are presented with respect to the instantaneous SNR as defined in (6).

In the results that follow, the HPD region is computed using the posterior distribution in (13) for AWGN channels and the approximate posterior distribution in (15) for multipath

[2]We use $\overset{\propto}{\sim}$ to denote that the right hand side is proportional to an approximation of the likelihood function.

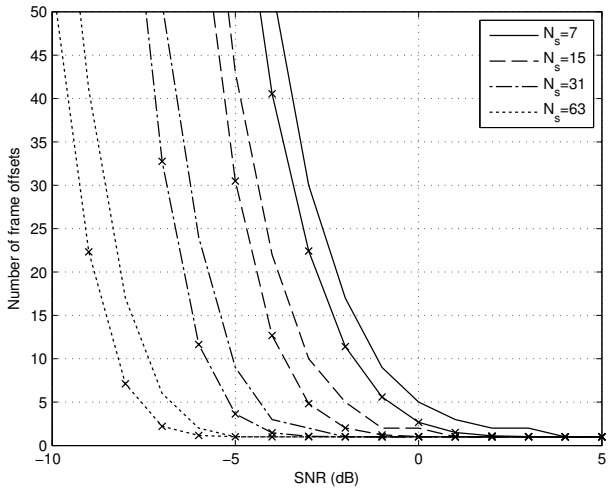

Fig. 3. Mean number of frame offsets in the $(1 - 10^{-3})$ HPD region ("x" marker) and in a fixed size list (no marker) for an AWGN channel.

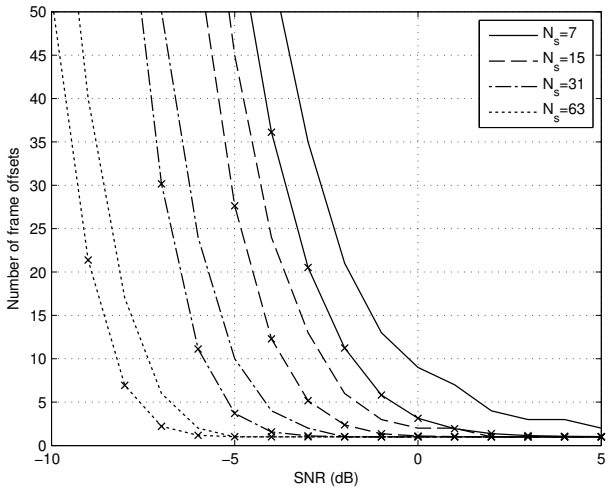

Fig. 4. Mean number of frame offsets in the $(1 - 10^{-3})$ HPD region ("x" marker) and in a fixed size list (no marker) for a multipath channel.

channels. The mean HPD region size for a probability of exclusion of $P_{ex} = 10^{-3}$ is shown for AWGN and multipath in Figs. 3 and 4, respectively. The HPD region is compared to list synchronization [11], [15] in Figs. 3 and 4 by determining, through simulation, the required size of a fixed size list to achieve the same target P_{ex}.

Remark 1. Using the HPD region reduces the complexity by a factor of 2-3 over list based synchronization and can guarantee a P_{ex} value without requiring simulations to tune the list size.

The FSER of the uncoded MAP synchronizer and the P_{ex} achieved[3] by the HPD region are compared in Figs. 5 and 6 for AWGN and multipath channels, respectively. The uncoded MAP estimate is found by taking the maximum over the posterior distributions in (13) and (15) for AWGN and multipath, respectively. Because the channel is known, we expect the performance in the AWGN channel and the multipath channel to be similar. However, for short sync word lengths, the use of the approximate likelihood function for the multipath channel leads to a higher P_{ex} and FSER and a larger required fixed list size. It is seen that the size of the HPD region is also affected by this approximation although the impact on the achieved P_{ex} in the multipath channel is small.

Remark 2. In Fig. 6, there is only a slight degradation in the P_{ex} achieved by the HPD region (i.e., P_{ex} is slightly greater than 10^{-3}) due to the approximation made in the likelihood function for multipath channels. Thus, the approximation is useful for the purposes of the HPD region-based pre-processing stage.

Remark 3. As SNR increases, the P_{ex} of the HPD region improves below the target value. Since the uncoded MAP estimate is always included in the HPD region, the FSER of the uncoded MAP synchronizer provides an upper bound on the P_{ex}—although in these simulations the P_{ex} maintains an order of magnitude or more improvement.

Remark 4. There is a sharp transition in the HPD region size as a function of SNR. For each sync word length, the transition occurs at an SNR which is lower than that required for the uncoded MAP synchronizer to achieve the target P_{ex}.

We observe in Figs. 3 and 4 that a shorter sync word length increases the size of the HPD region. When the length of the sync word is reduced by (approximately) half, there is about a 2 dB loss for the mean size of the HPD region (see Figs. 3 and 4), while there is a 3 dB loss in the uncoded MAP synchronizer's performance (see Figs. 5 and 6). Thus, possible gains from code-aided frame synchronization versus conventional synchronization are greatest for short sync word lengths.

We conclude that the HPD region provides a useful tool in minimizing the complexity of the proposed iterative receiver. By comparing the HPD region size with the FSER of the uncoded MAP estimate, we can begin to identify a range of SNR over which the complexity of the iterative receiver is reasonable and the performance of a conventional receiver based on uncoded MAP synchronization does not reach the target. We will return to this idea in Section VII after considering the complexity of the code-aided algorithms.

VI. Code-Aided Synchronization

After the pre-processing stage, $\mathcal{S}$ (the set of frame offsets in the HPD region) is conveyed to the code-aided frame synchronization stage as shown in Fig. 1. This stage initiates code-aided frame synchronization (as described in this section) for each of the frame offsets in the HPD region as shown by the duplicate receiver chains in Fig. 1. While the code structure is ignored in the frame pre-processing stage, it is utilized in this stage in order to make the final frame offset estimate. After this estimate has been made, further processing is executed on the receiver chain corresponding to the selected frame offset in order to estimate the information bits.

[3]The achieved P_{ex} is different from the target P_{ex} due to the discrete number of frame offsets in the HPD region and the use of an approximate likelihood function in the case of multipath.

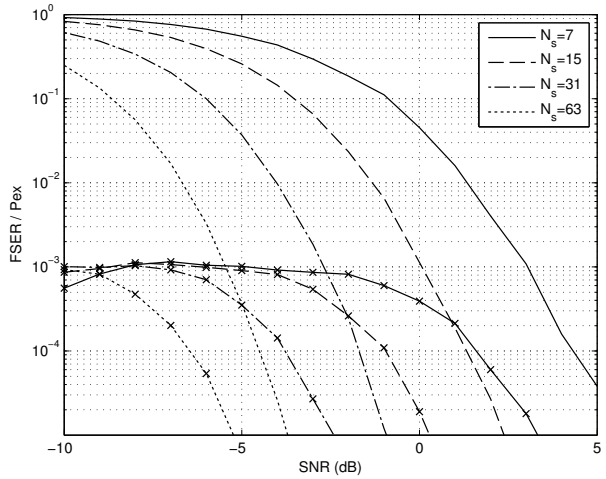

Fig. 5. Comparison between the FSER of the uncoded MAP estimate (no marker) and the achieved P_{ex} of the $(1 - 10^{-3})$ HPD region ("x" marker) for an AWGN channel.

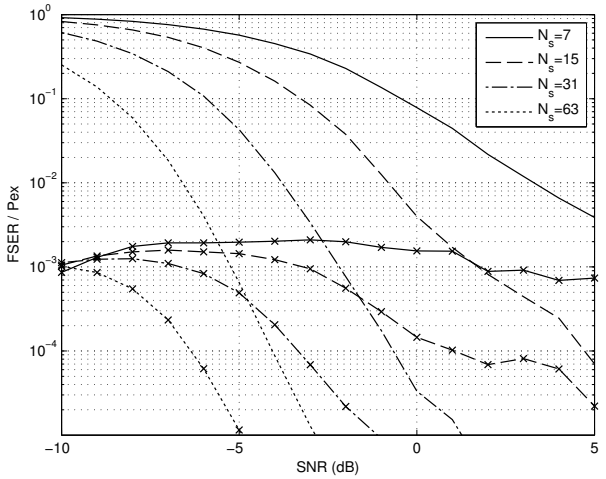

Fig. 6. Comparison between the FSER of the uncoded MAP estimate (no marker) and the achieved P_{ex} of the $(1 - 10^{-3})$ HPD region ("x" marker) for a multipath channel.

In this section, we present the following code-aided frame synchronization methods for the multipath channel:

- maximization of the syndrome posterior probability (SPP) of the code parity checks and
- approximate MAP hypothesis testing motivated by the EM algorithm.

A. SPP Algorithm

One of the properties of a linear code is the existence of a parity check matrix $\mathbf{H}$ which defines the dependencies between the coded bits. A binary sequence $\mathbf{c}$ is a valid codeword if it satisfies the parity check relations or, in other words, when the syndrome of the operation $\mathbf{Hc}$ is the all zeros vector. There are $N_p = N_c - N_b$ parity check relations represented by the rows of $\mathbf{H}$. Let the number of nonzero elements in the ith row of $\mathbf{H}$ be given by J_i and let $\phi_i(j)$ for all $j = 1, 2, \ldots, J_i$ provide the index of the jth nonzero element in the ith row of $\mathbf{H}$. The ith parity check relation is written as given by

$$c_{\phi_i(1)} \oplus c_{\phi_i(2)} \oplus \cdots \oplus c_{\phi_i(J_i)} = 0, \tag{16}$$

where $\oplus$ denotes modulus two addition.

The presence of the frame at an offset of η implies that the code structure is present in the received samples at this offset. Let $E_i(\eta)$ denote the event that the ith parity check is satisfied when the frame delay is given by η. Rather than approach the MAP estimator by applying Bayes' rule as in Section III, the posterior probability of η is equated to the joint probability that the parity checks are satisfied at an offset of η [23], [25]. Mathematically, this is expressed as given by

$$p(\eta|\mathbf{y}) = \mathrm{P}\left[\bigcap_{i=1}^{N_p} E_i(\eta)\Big|\mathbf{y}\right]. \tag{17}$$

An assumption of independence between the events is made as given by

$$p(\eta|\mathbf{y}) \approx \prod_{i=1}^{N_p} \mathrm{P}\left[E_i(\eta)|\mathbf{y}\right] \tag{18}$$

which has similarly been made by [23], [25].

The posterior probability of parity check $E_i(\eta)$ is given by

$$\begin{aligned}\mathrm{P}\left[E_i(\eta)|\mathbf{y}\right] &= \sum_{c_{\phi_i(1)}} \cdots \sum_{c_{\phi_i(J_i)}} \mathrm{P}\left[E_i(\eta), c_{\phi_i(1)}, \ldots, c_{\phi_i(J_i)}|\mathbf{y}\right] \\ &= \sum_{c_{\phi_i(1)}} \cdots \sum_{c_{\phi_i(J_i)}} \mathrm{P}\left[E_i(\eta)|c_{\phi_i(1)}, \ldots, c_{\phi_i(J_i)}\right] \\ &\quad \cdot p(c_{\phi_i(1)}, \ldots, c_{\phi_i(J_i)}|\mathbf{y})\end{aligned} \tag{19}$$

where the posterior probability of the coded bits is approximated as a multiplication of the coded bit likelihoods

$$p(c_{\phi_i(1)}, \ldots, c_{\phi_i(J_i)}|\mathbf{y}) \approx \prod_{j=1}^{J_i} p(\mathbf{y}|c_{\phi_i(j)}). \tag{20}$$

Converting these operations into the log domain, the logarithm of the posterior probability can be expressed as a function of the log-likelihood ratios (LLRs) of the coded bits. The logarithm of the event posterior probability is given by

$$\ln \mathrm{P}\left[E_i(\eta)|\mathbf{y}\right] = -\ln(1 + e^{-\gamma_i(\eta)}) \tag{21}$$

where $\gamma_i(\eta)$ is the log-likelihood ratio for the ith event $E_i(\eta)$. In this case, $\gamma_i(\eta)$ is given by the box-plus operation [33]

$$\gamma_i(\eta) = \lambda_{\phi_i(1)}(\eta) \boxplus \lambda_{\phi_i(2)}(\eta) \boxplus \cdots \boxplus \lambda_{\phi_i(J_i)}(\eta) \tag{22}$$

where $\lambda_{\phi_i(j)}(\eta)$ is the log-likelihood ratio for $c_{\phi_i(j)}$. Simplifications to the box-plus operation enable efficient computation of the syndrome probability without significant loss in performance [25], [33].

Substituting (21) into (18), we approximate the logarithm of the posterior event probability $\ln p(\eta|\mathbf{y})$ by

$$\Lambda_{\mathrm{SPP}}(\eta) = -\sum_{i=1}^{N_p} \ln(1 + e^{-\gamma_i(\eta)}) \tag{23}$$

and the estimate of the frame offset is given by

$$\hat{\eta}_{\mathrm{SPP}} = \arg\max_{\eta \in \mathcal{S}} \Lambda_{\mathrm{SPP}}(\eta). \tag{24}$$

The method requires computing the log-likelihood ratio of each coded bit in the presence of intersymbol interference from multipath. In order to compute the coded bit log-likelihood ratios, we begin by computing the likelihood function of the symbols. In the case of an AWGN channel, the symbol likelihoods are given by

$$p(\mathbf{y}|a_i,\eta) \propto \exp\left\{-\frac{1}{\sigma^2}|y_{i+\eta+N_s} - h_0 a_i|^2\right\}. \tag{25}$$

In the case of a multipath channel the computation of the symbol likelihoods can be performed by using the BCJR algorithm [31]. However, to keep the complexity of this method low, we propose a linear minimum mean square error (MMSE) equalizer followed by computation of the symbol likelihoods given the equalizer output. MMSE equalization is performed once and the output is used for all frame offsets in the HPD region. Let the output of the equalizer be given by $\hat{x}_{\eta+k}$ for all $k = 0,\ldots,K-1$ and $\eta \in \mathcal{S}$. The symbol likelihoods are given by

$$p(\mathbf{y}|a_i,\eta) \approx p(\hat{x}_{i+\eta+N_s}|a_i) \propto \exp\left\{-\frac{1}{\sigma^2}|\hat{x}_{i+\eta+N_s} - a_i|^2\right\}. \tag{26}$$

Soft demodulation is performed to compute the coded bit LLRs from the symbol likelihoods. Let the function $\psi(i)$ return the index of the coded data symbol $a_{\psi(i)}$ corresponding to the ith coded bit. For example, $\log_2(M)$ coded bits including c_i are modulated to generate symbol $a_{\psi(i)}$. The coded bit log-likelihood ratio is given by

$$\lambda_i(\eta) = \ln \frac{\sum_{a_{\psi(i)}\in\mathcal{A}^0} p(\mathbf{y}|a_{\psi(i)},\eta)}{\sum_{a_{\psi(i)}\in\mathcal{A}^1} p(\mathbf{y}|a_{\psi(i)},\eta)} \tag{27}$$

where $\mathcal{A}^0$ and $\mathcal{A}^1$ denote subsets of the symbol alphabet for which $c_i = 0$ and $c_i = 1$, respectively.

In summary, the SPP algorithm is implemented by computing symbol estimates using an MMSE equalizer, the symbol likelihoods from (26), and the coded bit LLRs from (27). These operations are performed once to evaluate the coded bit LLRs necessary for all the frame offsets in the HPD region. The parity check LLRs for a given frame offset in $\mathcal{S}$ are computed from (22) using the coded bit LLRs corresponding to that offset. Finally, the SPP metric is computed from (23) and the maximum is taken as the frame offset estimate as shown in (24). A diagram of this procedure is shown in Fig. 7. Subsequently, the iterative receiver is used to recover the information bits at this frame offset.

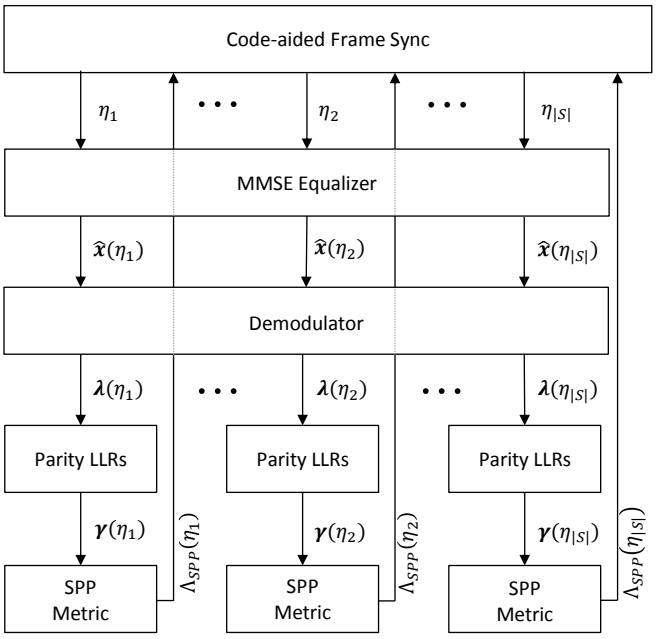

Fig. 7. SPP code-aided frame synchronization block diagram. The HPD region is labeled $\eta_1,\ldots,\eta_{|S|}$. The vectors $\hat{\mathbf{x}}(\eta_i)$, $\boldsymbol{\lambda}(\eta_i)$, and $\boldsymbol{\gamma}(\eta_i)$ are the symbol estimates, coded bits LLRs, and parity check LLRs, respectively, for frame offset η_i.

B. EM-Based Algorithm

The EM algorithm [34] provides a means of iteratively estimating parameter η from incomplete data $\mathbf{y}$ when there exists a set of unobserved or missing data $\mathbf{x}$. Maximization is performed on the complete data $\mathbf{z} = [\mathbf{y},\mathbf{x}]$ which typically simplifies computation. The EM algorithm is given by the following expectation (E) and maximization (M) steps:

$$\begin{aligned}&\text{E step: } Q(\eta,\hat{\eta}^{(p-1)}) = \int_{\mathbf{z}} p(\mathbf{z}|\mathbf{y},\hat{\eta}^{(p-1)}) \ln p(\mathbf{z}|\eta) d\mathbf{z}\\ &\text{M step: } \hat{\eta}^{(p)} = \arg\max_{\eta} Q(\eta,\hat{\eta}^{(p-1)})\end{aligned} \tag{28}$$

where p is the iteration number. However, the EM algorithm is not equipped to handle discrete parameters which has motivated a modification proposed by Wymeersch *et al.* where the expectation step is computed for all discrete values [17]. The EM-motivated algorithm is given a more rigorous mathematical explanation in [18] where it is shown to be an approximation to MAP hypothesis testing.

The discrete EM method is formulated for the frame synchronization problem as follows:

$$\hat{\eta}_{\text{EM}} = \arg\max_{\eta\in\mathcal{S}} Q(\eta) \tag{29}$$

where

$$Q(\eta) = \sum_{\mathbf{x}} p(\mathbf{x}|\mathbf{y},\eta) \ln p(\mathbf{y}|\mathbf{x},\eta). \tag{30}$$

As given in (29), maximization is performed over all frame offsets in the HPD region $\mathcal{S}$. The EM motivated algorithm computes the expectation of the log-likelihood function with respect to the data symbols rather than performing marginalization over the data symbols as required in the MAP estimator given in (8).

In the case of an AWGN channel, the log-likelihood $\ln p(\mathbf{y}|\mathbf{x},\eta)$ from (30) can be simplified as given by

$$\ln p(\mathbf{y}|\mathbf{x},\eta) \propto \sum_{i=0}^{K+L-2} \frac{2}{\sigma^2} \Re\left[y^*_{i+\eta} h_0 x_i\right] - \frac{1}{\sigma^2}|h_0 x_i|^2. \tag{31}$$

Substituting (31) into (30) and rearranging the summations

provides the following expression for the expectation step:

$$Q(\eta) = \sum_{i=0}^{K+L-2} \frac{2}{\sigma^2} \Re \left[y_{i+\eta}^* h_0 \sum_{x_i} x_i^* p(x_i|\mathbf{y}, \eta) \right] - \frac{1}{\sigma^2} |h_0|^2 \sum_{x_i} |x_i|^2 p(x_i|\mathbf{y}, \eta). \quad (32)$$

We observe that the EM framework has reduced the summation over coded symbol sequences in (30) to symbol-by-symbol summations.

In the case of ISI from a multipath channel, the log-likelihood is given by

$$\begin{aligned} &\ln p(\mathbf{y}|\eta, \mathbf{x}) \\ &\propto \sum_{i=0}^{K+L-2} \frac{2}{\sigma^2} \Re \left[y_{i+\eta}^* \left(\sum_{l=\alpha_i}^{\beta_i} h_l x_{i-l} \right) \right] - \frac{1}{\sigma^2} \left| \sum_{l=\alpha_i}^{\beta_i} h_l x_{i-l} \right|^2 \\ &\propto \frac{2}{\sigma^2} \Re \left[\sum_{i=0}^{K-1} x_i \sum_{l=0}^{L-1} y_{i+l+\eta}^* h_l \right] \\ &\quad - \frac{1}{\sigma^2} \sum_{i=0}^{K+L-2} \sum_{l_1=\alpha_i}^{\beta_i} \sum_{l_2=\alpha_i}^{\beta_i} h_{l_1} h_{l_2}^* x_{i-l_1} x_{i-l_2}^*. \end{aligned} \quad (33)$$

Substituting (33) into (30), evaluation requires marginal posterior probabilities of the symbols $p(x_i|\eta, \mathbf{y})$ as well as pairwise joint posterior probabilities $p(x_i, x_j|\eta, \mathbf{y})$. Thus, the complexity has been reduced to being linear in the codeword length as a result of the EM-motivated approximation. The sync word is naturally included in this method where the posterior probabilities associated with the sync symbols are unit impulses.

The posterior probabilities for the coded data symbols are obtained from the decoder. Thus, the EM-based method requires decoding all frame offsets in the HPD region. The receiver performs iterative MAP equalization and decoding based on the sum-product algorithm. Marginal and pairwise joint symbol posterior probabilities are estimated using the beliefs from the sum-product algorithm. Code-aided estimation of the other channel parameters may also be incorporated into the receiver framework as shown in Fig. 1. A viable alternative to the MAP equalizer is turbo equalization as proposed in [5] which reduces the computational complexity for large L.

VII. Numerical Results

A. Receiver Performance

Simulations are presented which quantify the performance and complexity of the frame synchronization methods. The frame is constructed from a 15 symbol m-sequence and a 1/4-rate LDPC codeword of length 2164 symbols. The modulation is BPSK and the target P_{ex} is set to 10^{-3}. The multipath channel has $L = 4$ taps with coefficients drawn from complex Gaussian random variables as described in Section V-B. In this section, we quantify the performance and complexity of the receiver under the assumption that all channel parameters other than the frame offset are known. In the next section, we will relax this assumption and include estimation of all channel parameters.

In Fig. 8, the FSER performance of the receiver is shown for the SPP and EM-based code-aided methods. The SPP frame synchronizer is based on the evaluation of (23) and decision of (24). The EM-based frame synchronizer is based on evaluation of (33), substituted into (30), and the decision of (29). Comparison is also made to a conventional receiver which performs frame synchronization with the uncoded MAP estimator, i.e., the use of (15) to approximate the argument of (8). In the case of the EM-based method, the receiver performs two iterations of the sum-product algorithm for each frame offset. The EM-based algorithm makes use of the sync word in addition to the code structure. Thus, the performance of this method converges to the uncoded MAP synchronization (i.e., conventional) performance at low SNR.

Although further iterations of the sum-product algorithm are required in order to reliably detect the data, good *synchronization* performance is seen with just two iterations for the EM-based algorithm. The SPP method is less complex than the EM-based method, yet its performance is comparable (at moderate to high SNR). Due to the limitations of linear equalizers, if the MMSE equalizer output is used for data detection (i.e., decoding), the performance is poor. For example, losses of 3-5 dB are shown for the MMSE linear equalizer compared to a MAP equalizer in a non-iterative case [5]. However, when the MMSE linear equalizer is used for frame synchronization in the SPP method, a loss of 1 dB or less is observed with respect to the EM-based method.

The FER performance of the receiver with the EM-based synchronization method is compared to that of conventional (uncoded MAP) synchronization in Fig. 9. The FER in perfect synchronization is based on iterative MAP equalization and decoding with the sum-product algorithm. We observe in Fig. 9 that the FER of the proposed receiver is within 0.3 dB of the ideal performance at a FER of 10^{-3}. Further, the proposed receiver achieves a performance gain of about 3 dB over the conventional receiver. We observe in Fig. 9 that the frame synchronization performance of the EM-based method is not the limiting factor in the FER performance of the receiver. The same is not true of the conventional receiver. This performance improvement is achieved by computing the expectation in (30) for each frame offset in the HPD region. Therefore, an understanding of the complexity can be gained by observing the mean number of frame offsets in the HPD region for $N_s = 15$, found in Fig. 4. For example, at SNR $= -3$ dB, the mean HPD region size is $|\mathcal{S}| = 5.2$.

B. Complexity

The complexity of the SPP method and of a single iteration of decoding are both $O(N_p)$. In the case of the EM-based method, two iterations of the sum-product algorithm were performed in order to compute the required posterior probabilities. As a benchmark, we consider a conventional receiver which processes a single frame offset and performs 20 iterations of the sum-product algorithm for data detection. Let Z denote the complexity of a single iteration of the sum-product algorithm based equalizer, demodulator, and decoder. Thus, $20Z$ is the complexity of the conventional receiver. The complexity of

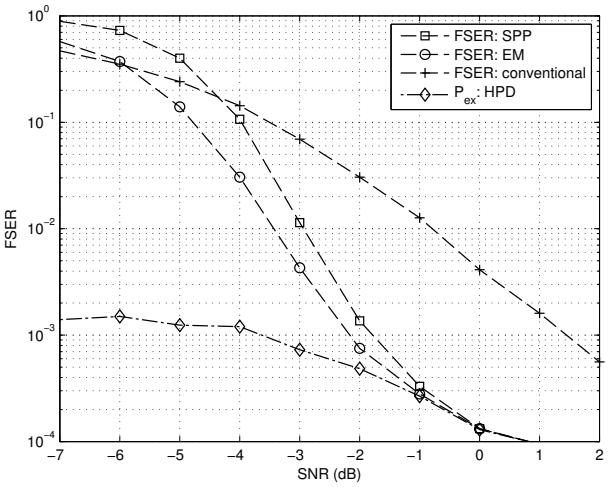

Fig. 8. FSER vs. instantaneous SNR of the code-aided frame synchronization methods for a multipath channel.

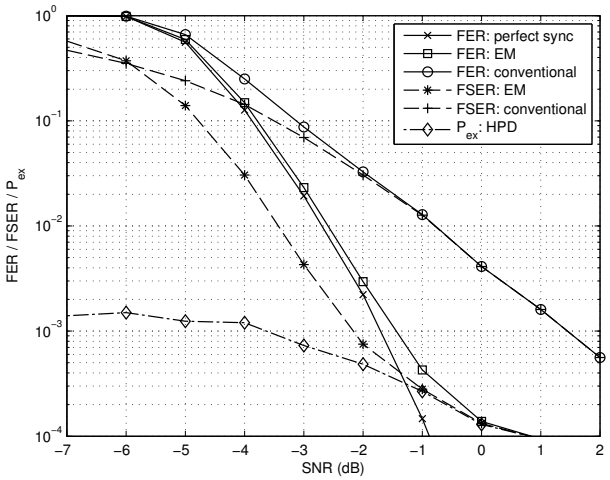

Fig. 9. FER vs. instantaneous SNR of the proposed receiver with the EM-based code-aided frame synchronization method for a multipath channel. Note that E_b/N_0 = SNR + 6 dB.

the SPP-based receiver is $(|\mathcal{S}| + 20)Z$ and the complexity of the EM-based receiver is $(2|\mathcal{S}| + 20)Z$. Expressed as a multiple of the conventional receiver's complexity, the SPP and EM complexities are $\frac{|\mathcal{S}|}{20} + 1$ and $\frac{|\mathcal{S}|}{10} + 1$, respectively. For example, for an HPD region size of $|\mathcal{S}| = 5$, the complexity of the SPP method is 1.25× the complexity of the conventional receiver and the complexity of the EM-based method is 1.5× the complexity of the conventional receiver. The complexity of the proposed receiver is shown in Fig. 10 as a multiple of the conventional receiver's complexity. We observe that the complexity of the receiver based on each of the code-aided methods is very reasonable, especially in the operating region of the code. For example, when the FER of the iterative receiver approaches the target of 10^{-3} at an SNR of -2 dB, the complexity is a factor of 1.1× and 1.2× for the SPP and EM-based methods, respectively.

C. Low-SNR Synchronization Performance

In a wireless communication system we desire to support ACK/NACK and hybrid ARQ protocols even when the frame cannot be decoded. This goal motivates improving frame synchronization at low SNR values. For example, in a hybrid ARQ system with soft combining, additional parity bits can be transmitted when the initial message was not successfully decoded. In order to combine the additional parity bits with the original message, frame synchronization must be obtained even when the frame is not decoded properly. In Fig. 11, the FSER of the SPP code-aided method is shown for five codeword lengths in both AWGN and multipath channels. In this simulation, the code is a 1/2-rate LDPC code, the modulation is BPSK, and the frame is transmitted without a sync word. As a point of reference, the channel capacity for binary signaling in AWGN is shown in Fig. 11. In either channel, every time the codeword length is doubled, the performance of the synchronization algorithm improves by about 1 dB. The results demonstrate the ability of the code-aided method to perform synchronization below the SNR required for recovery of the information bits. Even when accurate decoding is not possible, if a sufficient number of parity checks are likely to be satisfied at the true offset, accurate frame synchronization is possible.

D. Value of Code-Aided Synchronization

As discussed in Section VII-B, the complexity of the proposed receiver depends on the size of the HPD region as well as the computational requirements of the chosen frame synchronization method. Now that we have considered the complexity of the code-aided methods, we interpret the results in Figs. 3 and 4 in light of their impact on the complexity and value of the proposed receiver. We consider the proposed receiver to provide value over the conventional receiver when (a) the proposed receiver achieves the target performance while the conventional does not and (b) the complexity of the proposed receiver is within a factor of 2× the complexity of the conventional receiver.

The conventional receiver performs 10 and 20 decoder iterations in the AWGN and multipath channels, respectively. For the EM-based code-aided method, one and two iterations are performed in the AWGN and multipath channels, respectively. The value of SNR at which the complexity falls below a factor of 2 (with respect to a conventional receiver) is recorded in Table I. In addition, the value of SNR at which the FSER of the uncoded MAP estimator reaches the target performance (10^{-3}) is recorded in Table I. Even when the conventional receiver reaches the target performance, the code-aided methods may continue to provide an improvement in performance as observed in Figs. 5 and 6, but additional gains might not be needed.

Remark 5. Table I provides regions of SNR where the code-aided methods outperform conventional frame synchronization while maintaining a reasonable complexity. For a given amount of overhead, due to the sync word, the proposed receiver is capable of operating at an SNR which is anywhere from 2.8 to 10.2 dB below that of the conventional receiver.

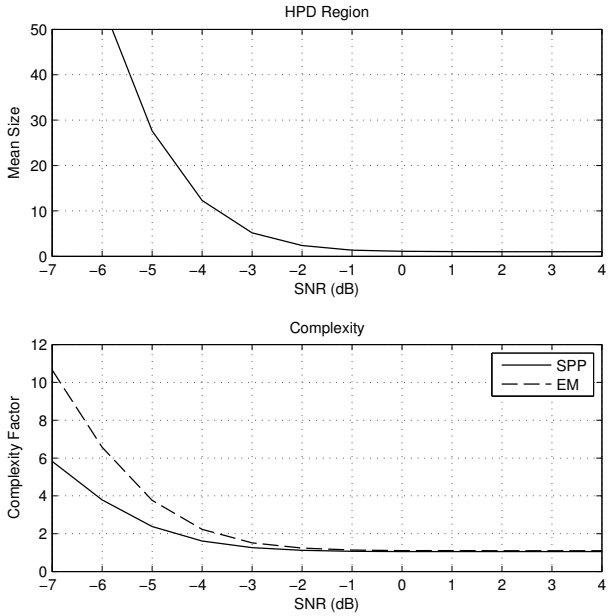

Fig. 10. Number of frame offsets in the HPD region and the resulting complexity of the proposed SPP and EM-based receivers (relative to the conventional receiver) for a multipath channel.

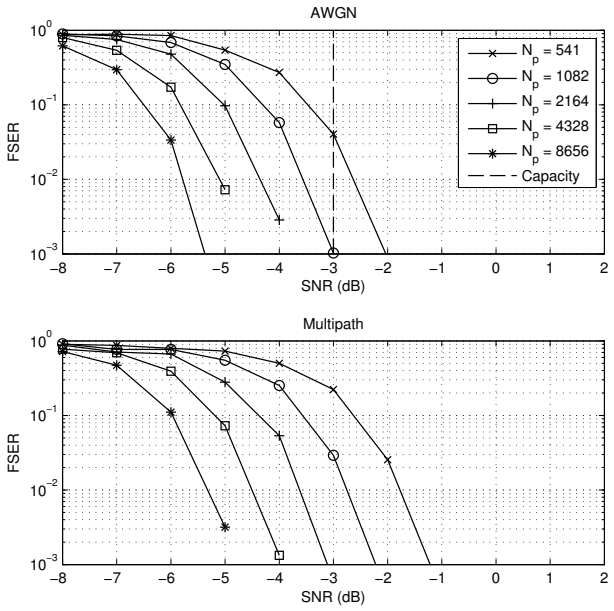

Fig. 11. FSER of the SPP code-aided frame synchronization method for five codeword lengths in an AWGN channel and a multipath channel ($\mathbf{h} = [\,-0.09 - 0.53j,\ 0.60 - 0.34j,\ 0.17 + 0.20j,\ 0.01 - 0.42j\,]^{\mathrm{T}}$). Note that $E_b/N_0 = \mathrm{SNR} + 3$ dB.

When comparing the proposed receiver to the conventional receiver, the most substantial gains are observed in the multipath channel. Since, the conventional receiver estimates the frame offset using the uncoded signal model, the approximation made in the likelihood function in (15) has a more pronounced impact on the performance. As the length of the sync word increases, the presence of multipath in the channel does not substantially impact either receiver. We see that the proposed receiver begins to behave very similarly in AWGN and multipath channels as the sync word length increases. With the length 63 m-sequence, the proposed receiver remains capable of providing a significant performance improvement over the conventional receiver (≥ 2.8 dB). The choice of sync word impacts the size of the HPD region and determines the regions of SNR over which the proposed receiver provides value, as given in Table I. The choice of code rate and modulation will determine the desired operating SNR of the receiver and thus will also indirectly impact the complexity of the proposed receiver.

TABLE I
REGIONS OF VALUE FOR THE PROPOSED RECEIVER (VALUES IN dB)

AWGN Channel		
N_s	SPP & EM	Conventional
(m-seq. length)	(SNR for complexity $\leq 2\times$)	(SNR for FSER $\leq 10^{-3}$)
7	-1.8	3.0
15	-3.8	0.1
31	-5.9	-2.7
63	-8.3	-5.5

Multipath Channel			
N_s	SPP	EM	Conventional
(m-seq. length)	(SNR for complexity $\leq 2\times$)		(SNR for FSER $\leq 10^{-3}$)
7	-3.0	-1.8	7.2
15	-4.6	-3.8	1.7
31	-6.6	-5.9	-2.2
63	-8.9	-8.3	-5.2

VIII. Extension to an Unknown Channel

In this section we consider the case of unknown channel and noise parameters. The two purposes of this extension are (a) to integrate code-aided frame synchronization into an iterative receiver structure for synchronization, channel estimation, equalization, demodulation, and decoding and (b) to show the impact of imperfect channel information on the frame pre-processing stage. Before the frame pre-processing stage, non-data-aided (blind) channel estimation is used to obtain coarse estimates of the channel and noise parameters.

Due to the rotational symmetry of common digital phase-amplitude modulations, a phase ambiguity will be unresolved by blind channel estimation. Therefore, the estimated channel taps will be equal to the true channel taps rotated by the phase ambiguity plus an error term as given by

$$\hat{\mathbf{h}} = \mathbf{h}e^{j\frac{2\pi}{\Psi}\psi} + \mathbf{e}, \tag{34}$$

where $\hat{\mathbf{h}}$ is the estimated channel, Ψ is the number of rotational symmetries in the modulation, $\psi \in \{0, \ldots, \Psi - 1\}$ is the phase ambiguity, and $\mathbf{e}$ is the estimation error. For phase shift keying (PSK) constellations, Ψ is equal to the modulation order and for quadrature amplitude modulation (QAM) constellations $\Psi = 4$.

The iterative receiver structure presented in Fig. 1 is used to perform joint estimation of the channel, symbol timing, frame timing, and noise power and detection of the information bits. The receiver performs the following functions: a) blind

coarse estimation of the continuous parameters (channel gain, phase offset, symbol timing, and noise power), b) computation of the HPD region to select the frame offsets processed by the iterative receiver, c) EM-based hypothesis testing of the discrete parameters (phase ambiguity and frame offset), d) EM fine estimation of the continuous parameters, and e) posterior symbol and bit probability computation using the sum-product algorithm. While we focus on the EM-based code-aided method in this section, a complementary receiver can be designed with the SPP algorithm.

A. Iterative Receiver Structure

Each function in the receiver is briefly described in the following:

a) Coarse estimation: We use blind estimators to obtain initial, coarse estimates of the channel coefficients $\mathbf{h}$, symbol timing ϵ, and noise power σ^2 as shown in the "Coarse Symbol Timing Est." and "Coarse Channel Est." blocks of Fig. 1. The Oerder and Meyr (O&M) timing detector [35], moment-based amplitude, phase, and noise power estimators for AWGN [36], and the blind multipath channel estimators of [37] are examples of potential coarse estimators.[4]

b) HPD region pre-processing: The computation of the HPD region is conditioned on the coarse estimates $\{\hat{\mathbf{h}}, \hat{\epsilon}, \hat{\sigma^2}\}$ in an analogous way to the quasi hybrid likelihood ratio approach taken for detection and classification problems [36]. The phase ambiguity may be handled in the pre-processing stage in one of two ways. The approach taken in our work is to perform marginalization over the phase ambiguity when computing the (uncoded) posterior distribution for the frame offset. This case is appropriate when there is no sync word present in the transmitted signal (which we consider in the results of this section). Alternatively, the HPD region may be computed for the joint (uncoded) posterior distribution of the frame offset and phase ambiguity. In this case, the "Frame Pre-processing" block of Fig. 1 is a pre-processing stage for both the frame and phase ambiguity.

c) Code-aided hypothesis testing: The code-aided frame synchronization block of the receiver in Fig. 1 is generalized to code-aided hypothesis testing. The EM-based code-aided method presented in Section VI-B is applied to both discrete parameters: the frame offset and the phase ambiguity. This requires computation of (33) and the associated symbol posterior probabilities for each combination of frame offset $\eta \in \mathcal{S}$ and phase ambiguity $\psi \in \{0, \ldots, \Psi - 1\}$. The fine channel estimates, discussed in the following bullet, are used in the evaluation of the code-aided metric. Fine estimates of the continuous parameters are obtained *per* hypothesis, making this a composite hypothesis test [39].

d) Fine channel estimation: Fine estimation of the continuous parameters $\mathbf{h}$, ϵ, and σ^2 is performed for each hypothesis $\{\eta, \psi\}$ as represented by the "Fine Channel Estimation" blocks in Fig. 1. We make use of the ECM algorithm, a variant of the EM algorithm, to sequentially perform maximization over each parameter while conditioning on the remaining parameters [29]. Posterior symbol probabilities required for code-aided hypothesis testing are also used for fine estimation of the continuous parameters which enables the fine estimation stage to be efficiently implemented.

e) Sum-product algorithm: The expectation step of both the EM-based hypothesis test and the ECM algorithm requires computation of the marginal symbol posterior probabilities. Also, MAP bit-wise detection is performed using marginal posterior probabilities of the information bits. The sum-product algorithm performs efficient computation of these probabilities by applying message passing on a factor graph representation of the equalizer, demodulator, and decoder shown in Fig. 1.

B. Numerical Results

The performance of the proposed iterative receiver in the presence of an unknown AWGN channel is evaluated for a transmission length of 1000 information bits, 16QAM modulation, and a 1/2-rate turbo code ($N_a = 500$). No sync word is included in the transmission, requiring the receiver to perform training-less recovery ($N_s = 0$, $K = 500$). The unknown parameters are h_0, ϵ, σ^2, ψ, and η. Energy detection is used to find the maximum energy frame offset of the received signal, and the domain of the frame offset is set relative to this point. We found $H = 51$ to be sufficiently large to ensure that the true offset is always included in the frame offset characterization. In order to minimize complexity without significant performance loss, the target P_{ex} was set to be 1/10th of the frame error rate achieved with perfect synchronization. For each hypothesis, 10 iterations of the ECM algorithm are performed, each of which includes a single iteration of the sum-product algorithm.

Simulation results of the FER are presented for four cases: (a) iterative demodulation and decoding with perfect synchronization (Perfect sync.); (b) hypothesis testing of ψ, η with no iterative estimation of the other parameters (HT); (c) the full iterative receiver with hypothesis testing and the ECM algorithm (HT/ECM); and (d) an iterative receiver with an uncoded MAP frame estimator (Uncoded MAP Frame Estimate). The performance of each case is shown in Fig 12. The iterative receiver demonstrates performance very near to that of perfect synchronization. In other words, the iterative receiver's ability to perform code-aided synchronization is on the same order as the decoder's ability to successfully decode the information in a known channel. Limiting the iterative receiver to only hypothesis testing results in a loss of 0.1-0.2 dB. The performance of the fourth case—considering only the uncoded MAP frame offset estimate—quickly becomes limited by frame synchronization errors.

In the iterative receiver, the frame offset posterior distribution is characterized using the coarse estimates of h_0, ϵ, and σ^2. In Fig. 12, the achieved P_{ex} for the iterative receiver performance simulation is shown. When the target P_{ex} is below 10^{-3}, we observe an increase in the probability of excluding the true frame offset from the HPD region as a

[4]The effect of a carrier frequency offset can be handled in the proposed receiver structure in a similar manner. For instance, coarse frequency synchronization is performed in the pre-processing stage using a blind estimator [38]. If necessary, residual frequency offset is removed using a code-aided approach in the fine channel estimation stage [6].

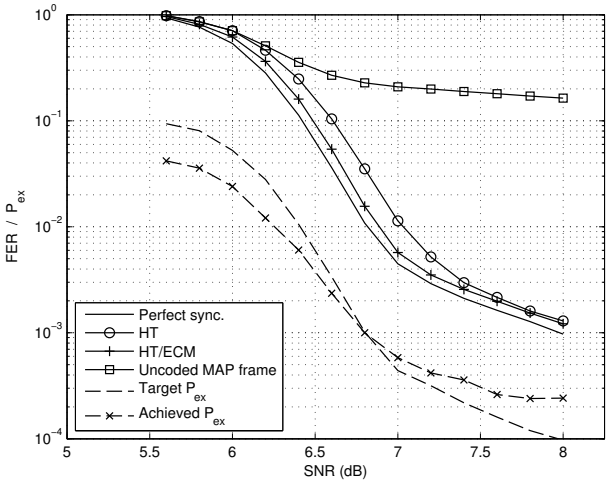

Fig. 12. Results for the FER for Perfect sync. (solid), HT (solid,circle), HT/ECM (solid,plus), and Uncoded MAP Frame Estimate (solid,square) as well as the target P_{ex} (dash) and the achieved P_{ex} (dash,'x') for the pre-processing stage of the HT and HT/ECM receivers. Note that E_b/N_0 = SNR – 3 dB.

result of errors in the coarse estimation stage, although the increase is slight.

Remark 6. The use of coarse estimates in the frame pre-processing stage slightly degrades the effectiveness of the HPD region. However, by setting the P_{ex} to 1/10th of the ideal FER, the decoder (rather than the HPD region) becomes the limiting factor in the receiver's performance.

To provide insight into limiting factors in the performance of the examined receivers, Table II lists the number of frame errors according to the source of the error at an SNR of 7 dB. The number of frame errors is shown by receiver type. Frame errors may originate from excluding the true frame offset from $\mathcal{S}$, choosing an incorrect hypothesis when the true offset has been included in $\mathcal{S}$, and incorrect detection of one or more information bits when the true hypothesis has been chosen. The first two cases (frame synchronization errors) generally lead to half the bits being in error (i.e., the bit error rate is significantly affected). The third case generally results in fewer bit errors.

In the pre-processing stage, the true offset was excluded from the HPD region in 30 simulations (out of a total of 47 683 total simulated frames), which affects both the HT and HT/ECM receivers. When the true offset is included, the HT/ECM receiver always selected the correct hypothesis (i.e., no frame synchronization errors) while the HT receiver chose an incorrect hypothesis in 32 simulations.

Remark 7. Fine estimation of the continuous parameters with the ECM algorithm enables more reliable estimation of the frame offset and phase ambiguity, and improves data detection.

IX. Conclusion

In this paper, we presented the development of (a) SPP and EM-based code-aided frame synchronization methods for multipath channels; (b) a novel frame pre-processing stage based on the HPD region; and (c) the HT/ECM iterative receiver structure which supports frame synchronization, channel estimation, equalization, demodulation, and decoding. Table I was a main result of the paper where it was shown that the proposed receiver is capable of operating at an SNR from 2.8 to 10.2 dB below that of the conventional receiver while maintaining a complexity within 2× the conventional receiver's complexity. The performance of the proposed receiver was demonstrated in a scenario in which a gain of about 3 dB was achieved with a complexity increase of only 20%. Finally, the proposed receiver design was shown to reliably operate without prior knowledge of the channel and noise parameters. In this case, fine estimation of the continuous parameters in the HT/ECM receiver improved the performance of code-aided frame synchronization and data detection. Overall, code-aided frame synchronization is shown to provide value over conventional techniques while introducing a reasonable increase in complexity.

TABLE II
Breakdown of Frame Errors by the Source of the Error

Receiver Type	Total No. Frame Errors†	$\eta_{\text{true}} \notin \mathcal{S}$	$\eta_{\text{true}} \in \mathcal{S}$	
		Exclusion from HPD	Wrong Hypothesis	Parameter Error & Noise
Perfect Sync.	200	0	0	200
HT	521	30	32	459
HT/ECM	254	30	0	224

†The total number of frames in the simulation is 47 683.

References

[1] D. Jakubisin, C. I. Phelps, and R. M. Buehrer, "Iterative joint detection, decoding, and synchronization with a focus on frame timing," in *Proc. IEEE Wireless Commun. and Netw. Conf.*, Istanbul, Turkey, Apr. 2014, pp. 446–451.

[2] D. Jakubisin and R. M. Buehrer, "On the complexity-performance trade-off in code-aided frame synchronization," in *Proc. IEEE 15th Workshop Signal Process. Advances Wireless Commun. (SPAWC)*, Toronto, Ontario, Jun. 2014, pp. 364–368.

[3] J. Hagenauer, "The turbo principle: Tutorial introduction and state of the art," in *Proc. Int. Symp. Turbo Codes and Related Topics*, 1997, pp. 1–11.

[4] A. P. Worthen and W. E. Stark, "Unified design of iterative receivers using factor graphs," *IEEE Trans. Inf. Theory*, vol. 47, no. 2, pp. 843–849, Feb. 2001.

[5] M. Tuchler, R. Koetter, and A. C. Singer, "Turbo equalization: principles and new results," *IEEE Trans. Commun.*, vol. 50, no. 5, pp. 754–767, May 2002.

[6] N. Noels, V. Lottici, A. Dejonghe, H. Steendam, M. Moeneclaey, M. Luise, and L. Vandendorpe, "A theoretical framework for soft-information-based synchronization in iterative (turbo) receivers," *EURASIP J. Wireless Commun. Netw.*, vol. 2005, no. 2, pp. 117–129, Apr. 2005.

[7] R. H. Barker, "Group synchronizing of binary digital systems," *Communication Theory*, pp. 273–287, 1953.

[8] J. L. Massey, "Optimum frame synchronization," *IEEE Trans. Commun.*, vol. 20, no. 2, pp. 115–119, Apr. 1972.

[9] G. Lui and H. Tan, "Frame synchronization for Gaussian channels," *IEEE Trans. Commun.*, vol. 35, no. 8, pp. 818–829, Aug. 1987.

[10] C. Herzet and L. Vandendorpe, "Code-aided ML ambiguity resolution," in *Proc. IEEE Int. Conf. Commun. (ICC)*, Jun. 2007, pp. 2900–2905.

[11] P. Robertson, "A generalized frame synchronizer," in *Conf. Rec. IEEE Global Telecommun. Conf. (GLOBECOM)*, Dec. 1992, pp. 365–369.

[12] ——, "Improving frame synchronization when using convolutional codes," in *Conf. Rec. IEEE Global Telecommun. Conf. (GLOBECOM)*, vol. 3, Nov. 1993, pp. 1606–1611.
[13] M. Howlader and B. Woerner, "Decoder-assisted frame synchronization for packet transmission," *IEEE J. Sel. Areas Commun.*, vol. 19, no. 12, pp. 2331–2345, Dec. 2001.
[14] J. Sodha, "Turbo code frame synchronization," *Signal Process. J., Elsevier*, vol. 82, no. 5, pp. 803–809, 2002.
[15] T. Cassaro and C. Georghiades, "Frame synchronization for coded systems over AWGN channels," *IEEE Trans. Commun.*, vol. 52, no. 3, pp. 484–489, Mar. 2004.
[16] J. Sun and M. Valenti, "Optimum frame synchronization for preamble-less packet transmission of turbo codes," in *Conf. Rec. Thirty-Eighth Asilomar Conf. Signals Syst. and Comput.*, 2004, pp. 1126–1130.
[17] H. Wymeersch, H. Steendam, H. Bruneel, and M. Moeneclaey, "Code-aided frame synchronization and phase ambiguity resolution," *IEEE Trans. Signal Process.*, vol. 54, no. 7, pp. 2747–2757, Jul. 2006.
[18] C. Herzet, H. Wymeersch, F. Simoens, M. Moeneclaey, and L. Vandendorpe, "MAP-based code-aided hypothesis testing," *IEEE Trans. Wireless Commun.*, vol. 7, no. 8, pp. 2856–2860, Aug. 2008.
[19] C. Herzet, K. Woradit, H. Wymeersch, and L. Vandendorpe, "Code-aided maximum-likelihood ambiguity resolution through free-energy minimization," *IEEE Trans. Signal Process.*, vol. 58, no. 12, pp. 6238–6250, Dec. 2010.
[20] H. Huh and J. Krogmeier, "A unified approach to optimum frame synchronization," *IEEE Trans. Wireless Commun.*, vol. 5, no. 12, pp. 3700–3711, Dec. 2006.
[21] D.-U. Lee, H. Kim, C. Jones, and J. Villasenor, "Pilotless frame synchronization for LDPC-coded transmission systems," *IEEE Trans. Signal Process.*, vol. 56, no. 7, pp. 2865–2874, Jul. 2008.
[22] C. Stefanovic, D. Vukobratovic, and D. Bajic, "Low-complexity list-based frame synchronization for LDPC coded transmission," in *Proc. IEEE Int. Conf. Commun. (ICC)*, Jun. 2009, pp. 1–5.
[23] R. Imad, G. Sicot, and S. Houcke, "Blind frame synchronization for error correcting codes having a sparse parity check matrix," *IEEE Trans. Commun.*, vol. 57, no. 6, pp. 1574–1577, Jun. 2009.
[24] R. Imad and S. Houcke, "Theoretical analysis of a MAP based blind frame synchronizer," *IEEE Trans. Wireless Commun.*, vol. 8, no. 11, pp. 5472–5476, Nov. 2009.
[25] R. Moosavi and E. Larsson, "Fast blind recognition of channel codes," *IEEE Trans. Commun.*, vol. 62, no. 5, pp. 1393–1405, May 2014.
[26] J. S. Yedidia, W. Freeman, and Y. Weiss, "Constructing free-energy approximations and generalized belief propagation algorithms," *IEEE Trans. Inf. Theory*, vol. 51, no. 7, pp. 2282–2312, Jul. 2005.
[27] P. Robertson, "Maximum likelihood frame synchronization for flat fading channels," in *Conf. Rec. IEEE Int. Conf. Commun. (ICC)*, vol. 3, Jun. 1992, pp. 1426–1430.
[28] B. Moon and S. Soliman, "ML frame synchronization for the Gaussian channel with ISI," in *Conf. Rec. IEEE Int. Conf. Commun. (ICC)*, vol. 3, Jun. 1991, pp. 1698–1702.
[29] X. L. Meng and D. B. Rubin, "Maximum likelihood estimation via the ECM algorithm: A general framework," *Biometrika*, vol. 80, no. 2, pp. 267–278, Jun. 1993.
[30] M. K. Simon and M.-S. Alouini, "A unified approach to the performance analysis of digital communication over generalized fading channels," *Proc. IEEE*, vol. 86, no. 9, pp. 1860–1877, Sep. 1998.
[31] L. Bahl, J. Cocke, F. Jelinek, and J. Raviv, "Optimal decoding of linear codes for minimizing symbol error rate (corresp.)," *IEEE Trans. Inf. Theory*, vol. 20, no. 2, pp. 284–287, Mar. 1974.
[32] F. R. Kschischang, B. J. Frey, and H. A. Loeliger, "Factor graphs and the sum-product algorithm," *IEEE Trans. Inf. Theory*, vol. 47, no. 2, pp. 498–519, Feb. 2001.
[33] J. Hagenauer, E. Offer, and L. Papke, "Iterative decoding of binary block and convolutional codes," *IEEE Trans. Inf. Theory*, vol. 42, no. 2, pp. 429–445, Mar. 1996.
[34] A. P. Dempster, N. M. Laird, and D. B. Rubin, "Maximum likelihood from incomplete data via the EM algorithm," *J. Roy. Stat. Soc., Ser. B*, vol. 39, no. 1, pp. 1–38, Jan. 1977.
[35] M. Oerder and H. Meyr, "Digital filter and square timing recovery," *IEEE Trans. Commun.*, vol. 36, no. 5, pp. 605–612, May 1988.
[36] A. Abdi, O. Dobre, R. Choudhry, Y. Bar-Ness, and W. Su, "Modulation classification in fading channels using antenna arrays," in *Proc. 2004 IEEE Military Commun. Conf. (MILCOM)*, vol. 1, 2004, pp. 211–217.
[37] L. Tong and S. Perreau, "Multichannel blind identification: from subspace to maximum likelihood methods," *Proc. IEEE*, vol. 86, no. 10, pp. 1951–1968, Oct. 1998.
[38] U. Mengali and A. N. D'Andrea, *Synchronization techniques for digital receivers*. New York: Plenum Press, 1997.
[39] S. M. Kay, *Fundamentals of Statistical Signal Processing: Detection Theory*. Prentice-Hall, 1998.

Daniel J. Jakubisin (S'05–M'07) received the B.S. degree in 2006 from the University of North Carolina at Charlotte, Charlotte, NC, USA and the M.S. degree in 2013 from Virginia Polytechnic Institute and State University (Virginia Tech), Blacksburg, VA, USA, both in electrical engineering. He has continued at Virginia Tech where he is currently pursuing the Ph.D. degree with the Mobile and Portable Radio Research Group (MPRG) within Wireless @ Virginia Tech. His research interests include iterative receiver design, communication theory, statistical signal processing, probabilistic graphical models, and machine learning.

R. Michael Buehrer (S'89–M'91–SM'04) joined Virginia Tech from Bell Labs as an Assistant Professor with the Bradley Department of Electrical and Computer Engineering in 2001. He is currently a Professor of Electrical Engineering and is the director of *Wireless @ Virginia Tech*, a comprehensive research group focusing on wireless communications. During 2009 Dr. Buehrer was a visiting researcher at the Laboratory for Telecommunication Sciences (LTS) a federal research lab which focuses on telecommunication challenges for national defense. While at LTS, his research focus was in the area of cognitive radio with a particular emphasis on statistical learning techniques.

His current research interests include geolocation, position location networks, iterative receiver design, electronic warfare, dynamic spectrum sharing, cognitive radio, communication theory, Multiple Input Multiple Output (MIMO) communications, intelligent antenna techniques, Ultra Wideband, spread spectrum, interference avoidance, and propagation modeling. His work has been funded by the National Science Foundation, the Defense Advanced Research Projects Agency, Office of Naval Research, and several industrial sponsors.

Dr. Buehrer has authored or co-authored over 50 journal and approximately 150 conference papers and holds 11 patents in the area of wireless communications. He was co-recipient of the *Fred W. Ellersick MILCOM Award* for the best paper in the unclassified technical program in 2010 and the Outstanding Paper Award from the SDR Forum Technical Conference in 2008. He is currently a Senior Member of IEEE and an Associate Editor for both IEEE TRANSACTIONS ON WIRELESS COMMUNICATIONS and IEEE WIRELESS COMMUNICATIONS LETTERS. He was formerly an Associate Editor for IEEE TRANSACTIONS ON VEHICULAR TECHNOLOGY, IEEE TRANSACTIONS ON COMMUNICATIONS, IEEE TRANSACTIONS ON SIGNAL PROCESSING, and IEEE TRANSACTIONS ON EDUCATION. In 2003, he was named Outstanding New Assistant Professor by the Virginia Tech College of Engineering and received the Dean's Award for Teaching Excellence in 2014.